Geometry, Symmetries, and Quantization of Scalar Fields in de-Sitter Space-time

Arpan Dey, Riddhiman Bhattacharya, Sanchari Sen

Abstract

The paper commences by examining the geometric properties of de-Sitter space-time, with a specific focus on the isometries generated by Killing vectors. It also investigates various metrics that are applicable to specific regions of space-time, revealing that in the distant future, the symmetries exhibit a similar local structure to that of $\mathbb{R}^3$. Furthermore, the classical Klein-Gordon equation is solved within this space-time, leading to the discovery that energy is not conserved. The solutions to the Klein-Gordon equation yield intriguing outcomes that have the potential to enable observations from the early inflationary era. Finally, the primary objective of the paper is to comprehensively examine a quantized scalar field in the de-Sitter background, exploring the solutions for the two-point function and analyzing their behavior during both early and late time periods.

Contents

1 Introduction

We initially delve into the motivation behind exploring quantum fields in de-Sitter space. While investigating abstract mathematical concepts can often provide unforeseen insights into various areas of physics, there are specific unexplored domains in mathematics and physics that hold significant physical value, allowing us to gain a deeper understanding of the universe we inhabit. Experimental observations demonstrate that our universe is not only expanding but expanding at an accelerating rate [1, 2]. This accelerated expansion is driven by a small, positive cosmological constant [3]. If this cosmological constant remains positive, it'll eventually lead to the dilution of the large-scale structure we observe today, giving rise to the popularly known scenarios of the "**big chill**" or "**big freeze**" [4].
Additionally, the inflationary era following the Big Bang also showcases the expansion of our universe [5, 6]. Some inflationary models incorporate a scalar field, which can be influenced by quantum fluctuations. Therefore, considering these two periods of expansion during which our universe exhibits approximate de-Sitter characteristics, it becomes evident why it's important to study the geometry of de-Sitter space and the effects of quantum interactions within such a framework.
Hence, the main objective of this paper is to establish a fundamental understanding of the nature of de-Sitter space-time, followed by the presentation of a quantum field theory formulated within this background. By comparing the solutions obtained in de-Sitter space with those in flat space-time, we aim to establish a foundation for further exploration and analysis.

2 de-Sitter spacetime

We'll start by looking at the geometry of the sphere, then identify the similarities shared with the de-Sitter geometry to gain a better understanding of the background spacetime [7] that I'm working in.

2.1 dS_2

Initially, We'll look at the geometry in dS_2 as it's easier to understand the concepts in lower dimensions, and then it becomes quite intuitive to generalize to higher dimensions; the space-time we're working toward understanding is dS_4.

2.1.1 Killing vectors

Killing vectors are generated by isometries and can be found by solving the Killing equation [8]

$$(\mathcal{L}_X g)_{ij} \coloneqq X^k \partial_k g_{ij} + \partial_i X^l g_{lj} + \partial_j X^l g_{li} = 0$$

where $\mathcal{L}$ is the Lie derivative, X is the Killing vector field and g is the metric. However, it can get quite complicated to solve the Killing equation for certain metrics, which is why we can make it easier to find the Killing vectors by transforming coordinates from a system where we already know the Killing vectors to our desired system, rather than repeatedly solving the Killing equation. To demonstrate this we can look at the simple example of the standard metric and the round metric on $\mathbb{R}^3$.
The standard metric on $\mathbb{R}^3$ is $ds^2 = dx^2 + dy^2 + dz^2$, so $g_{ij} = \delta_{ij}$, it's not difficult to find the Killing vectors which can be presented in the basis

$$\partial_i \tag{2.1}$$

$$\epsilon_{ijk} x^i \partial^j \tag{2.2}$$

where, $i = 1, 2, 3$ and repeated indices are summed. We note that the commutators of these Killing vector fields close on itself, and so it forms a Lie group which is that of the special Euclidean group. The first 3 Killing vectors Eq. (2.1) represent translations, and the second 3 Eq. (2.2) represent rotations. As mentioned earlier, isometries generate Killing vectors. The definition of an isometry is a coordinate transformation that leaves the metric unchanged because it is obvious that the distance between 2 points in $\mathbb{R}^3$ doesn't change under translations or rotations, they're intuitively Killing vectors.
The maximal number of Killing vectors in d-dimensions is $\frac{d(d+1)}{2}$, meaning for $\mathbb{R}^3$ there are 6, and as we've found 6, $\mathbb{R}^3$ is therefore maximally symmetric.

2.1.2 Classical geometry of the sphere

We'll now take a look at the geometry of the sphere. The equation for the unit sphere is given by $x^2 + y^2 + z^2 = 1$, our aim is to embed the coordinates onto the sphere, we proceed by changing to polar coordinates

$$x = R\cos\theta\cos\phi \tag{2.3}$$

$$y = R\cos\theta\sin\phi \tag{2.4}$$

$$z = R\sin\theta \tag{2.5}$$

where, $R = 1$ as we're looking at the unit sphere. We can then calculate the new metric by solving $dx^i = \frac{\partial x^i}{\partial\theta}d\theta + \frac{\partial x^i}{\partial\phi}d\phi$, where $x^i = \{x, y, z\}$, then substituting into the standard metric on $\mathbb{R}^3$, giving $ds^2 = d\theta^2 + \cos^2\theta d\phi^2$ commonly know as the **round metric on the 2-sphere**.

2.1.3 Isometries of the sphere

We notice that by embedding the coordinates onto the 2-sphere, we've reduced the dimensions by 1 as the 2-sphere is a 2 dimensional manifold, which means that we no longer have 6 Killing vectors, but 3 $\left(= \frac{2(2+1)}{2}\right)$.We find that by fixing the coordinates to the unit sphere the translations are no longer isometries, however, the rotations remain isometries of the 2-sphere and they form the special orthogonal group $SO(3)$ (note here, that the real isometry group of the sphere is $O(3)$, not $SO(3)$. However, $O(3)$ does not preserve chirality and there is no loss of generality in requiring that the determinant is $+1$, meaning we identify the group of isometries for the sphere as $SO(3)$, this assumption will be used throughout the rest of the paper for all isometry groups as we're not interested in the discrete symmetries). As previously mentioned, to calculate the Killing vectors of the 2-sphere we use the coordinate transformation from the standard metric as solving the Killing equation for the round metric becomes tedious.
First, we calculate the partial derivatives

$$\frac{\partial}{\partial x^i} = \frac{\partial\theta}{\partial x^i}\frac{\partial}{\partial\theta} + \frac{\partial\phi}{\partial x^i}\frac{\partial}{\partial\phi} \tag{2.6}$$

Which gives us

$$\frac{\partial}{\partial x} = -\sin\theta\cos\phi\frac{\partial}{\partial\theta} - \frac{\sin\phi}{\cos\theta}\frac{\partial}{\partial\phi} \tag{2.7}$$

$$\frac{\partial}{\partial y} = -\sin\theta\sin\phi\frac{\partial}{\partial\theta} + \frac{\cos\phi}{\cos\theta}\frac{\partial}{\partial\phi} \tag{2.8}$$

$$\frac{\partial}{\partial z} = \cos\theta\frac{\partial}{\partial\theta} \tag{2.9}$$

We, then, substitute into Eq. (2.2) the values for: x^i given by Eqs. (2.3) to (2.5), and ∂^j given by Eqs. (2.7) to (2.9), to give

$$x\partial_y - y\partial_x = \partial_\phi \tag{2.10}$$

$$y\partial_z - z\partial_y = \sin\phi\partial_\theta - \tan\theta\cos\phi\partial_\phi \tag{2.11}$$

$$z\partial_x - x\partial_z = -\cos\phi\partial_\theta - \tan\theta\sin\phi\partial_\phi \tag{2.12}$$

It is easy to show that these Killing vectors close under the Lie bracket.

2.1.4 de-Sitter geometry dS_2

As we've reviewed the simple example of spherical geometry, we now proceed in a similar way for the de-Sitter geometry. Instead of taking the standard metric on $\mathbb{R}^3$ though we look at the Minkowski metric $ds^2 = -dt^2 + dx^2 + dy^2$. It is obvious to see the similarity in the metrics as a simple coordinate transformation $t \to iz$ gives the standard metric. To discuss the reason for embedding the coordinates of the standard metric onto the 2-sphere, the de-Sitter geometry can be viewed as the embedding of the Minkowski metric onto the hyperboloid.

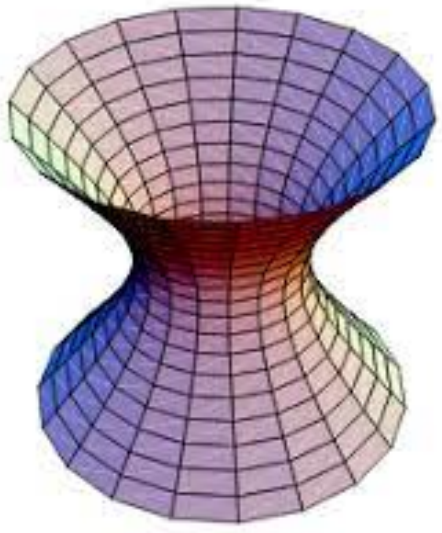

Figure 2.1: Hyperboloid surface

Proceeding in a similar fashion to the 2-sphere, we can start by identifying the Killing vectors of Minkowski spacetime $\mathbb{R}^{1,2}$. We realize the group structure we're looking for is the Poincaré group giving the Killing vectors

$$\partial_t \qquad \partial_x \qquad \partial_y \tag{2.13}$$

$$x\partial_t + t\partial_x \qquad\qquad y\partial_t + t\partial_y \tag{2.14}$$

$$x\partial_y - y\partial_x \tag{2.15}$$

we have 1-time translation and 2 spatial translations (2.13), 2 boosts (2.14) and 1 rotation (2.15) to give the 6 Killing vectors we expect of this 3-dimensional space-time. Following a similar procedure as before, taking the metric $ds^2 = -dt^2 + dx^2 + dy^2$ and embedding it onto the hyperboloid $-t^2 + x^2 + y^2 = 1$, using the coordinate transformations

$$t = \sinh T \tag{2.16}$$

$$x = \cosh T \cos\phi \tag{2.17}$$

$$y = \cosh T \sin\phi \tag{2.18}$$

we can calculate the new induced metric to be $ds^2 = -dT^2 + \cosh^2 T d\phi^2$ which is the de-Sitter metric dS_2, otherwise referred to as the global metric on dS_2. We notice that the only difference between this and the 2-sphere example is the simple coordinate transformation $z \to it$ and $\theta \to iT$ which highlights the similarities between the two geometries.

2.1.5 Isometries of dS_2

Now that, we've our Killing vectors on $\mathbb{R}^{1,2}$ and our embedding coordinates on the hyperboloid, we can look at finding the Killing vectors in dS_2. When embedding the coordinates, we again find that we lose the translation isometries leaving us with the rotation and two boosts, which are represented in this coordinate system, are

$$x\partial_y - y\partial_x = \partial_\phi \tag{2.19}$$

$$x\partial_t + t\partial_x = \cos\phi\partial_T - \sin\phi\tanh T\partial_\phi \tag{2.20}$$

$$y\partial_t + t\partial_y = \sin\phi\partial_T + \cos\phi\tanh T\partial_\phi \tag{2.21}$$

we identify this group as the Lorentz group in 2 spatial dimensions $SO(1,2)$.

2.1.6 Penrose diagram

We now take a look at the Penrose diagram, which is similar to the Minkowski space-time diagram in that the vertical direction represents time, the horizontal direction represents a spatial dimension, and the null geodesics are lines at 45°. The diagram is designed to capture the causal structure of the space-time, the difference to that of the Minkowski diagram is that, locally, the actual metric of the space-time is conformally equivalent to the metric on the diagram itself. This means the entire space-time is represented on the diagram, and so the coordinate system used has to be compact, which means we first need to compactify our coordinates.
We notice that for our metric $ds^2 = -dT^2 + \cosh^2 T d\phi^2$ the spatial coordinates ϕ are already compact, ranging from 0 to 2π. So, we only need to compactify the temporal coordinate, as T ranges from $-\infty$ to $+\infty$. We resolve this problem by changing coordinates, so the metric is of the form [9, 7]

$$ds^2 = a^2(\tau)(-d\tau^2 + d\phi^2) \tag{2.22}$$

We take our global metric and require

$$-dT^2 + \cosh^2 T d\phi^2 = a^2(\tau)(-d\tau^2 + d\phi^2) \tag{2.23}$$

Which gives us $a = \cosh T$ and $dT = a d\tau$ leading to

$$\int \frac{dT}{\cosh T} = \int d\tau \tag{2.24}$$

Which is solved to give

$$\tanh \frac{T}{2} = \tan \frac{\tau}{2} \tag{2.25}$$

If we then differentiate this to find dT in terms of $d\tau$ and τ, we get

$$dT = \frac{1}{\cos \tau} d\tau \tag{2.26}$$

Meaning the metric is now

$$ds^2 = \frac{1}{\cos^2 \tau}(-d\tau^2 + d\phi^2) \tag{2.27}$$

All our coordinates are now compact, as $\tanh x \in (-1, 1)$ for $x \in \mathbb{R}$, and $\tan^{-1} x \in (-\frac{\pi}{4}, \frac{\pi}{4})$ for $x \in (-1, 1)$, giving $\tau \in (-\frac{\pi}{2}, \frac{\pi}{2})$.
dS_2 is a special case for the **Penrose diagram** as the ϕ coordinate ranges from 0 to 2π, this means that the diagram has cylindrical topology as the spatial points 0 and 2π are the same. Horizontal lines, constant time τ slices are 1-spheres (circles), these 1-spheres shrink from $\mathcal{I}^-$ ($\tau = -\frac{\pi}{2}$) to 0 and expand from 0 to $\mathcal{I}^+$ ($\tau = \frac{\pi}{2}$).

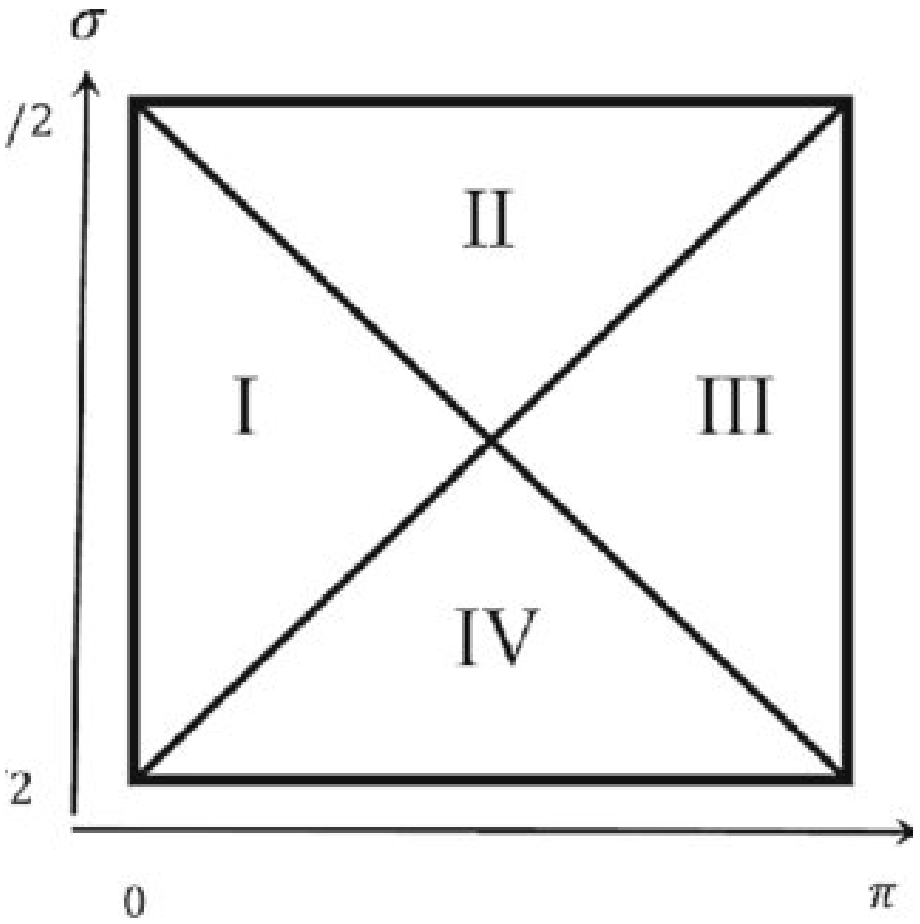

Figure 2.2: Penrose diagram dS_2

Looking at the causal structure of the diagram, if we place an observer at $\phi = \pi$, then from $\tau = -\frac{\pi}{2}$ the blue area is the region that they can influence, and at $\tau = \frac{\pi}{2}$, the red area is the region that can influence them. The purple area is the region which they can fully access which is called the **static patch**. The white area is the static patch for an observer at the other pole of the 1-sphere $\phi = 0$, this area is completely causally disconnected from the observer at $\phi = \pi$.

2.2 dS_4

Now, that we've reviewed dS_2 in detail we can look into the dimension, we're interested in which is dS_4. We'll follow a similar path to that of dS_2 by looking at the 4-sphere, and then, use a coordinate transformation to de-Sitter geometry to give a more intuitive perspective of the isometries.

2.2.1 de Sitter geometry dS_4

To begin, we again take the example of the sphere, but instead of using the 2-sphere, we'll now use the 4-sphere with radius l, which has equation $x^i x_i = l^2$ where i runs from 1 to

5. Taking the standard metric on $\mathbb{R}^5$, $ds^2 = dx^i dx_i$ and in the same way we did for the 2-sphere, we embed our coordinates onto the 4-sphere. Our embedding coordinates are as follows

$$x_1 = l\sin\phi_1 \qquad \phi_1 = \arctan\left(\frac{x_1}{\sqrt{x_2^2+x_3^2+x_4^2+x_5^2}}\right) \tag{2.28}$$

$$x_2 = l\cos\phi_1\sin\phi_2 \qquad \phi_2 = \arctan\left(\frac{x_2}{\sqrt{x_3^2+x_4^2+x_5^2}}\right) \tag{2.29}$$

$$x_3 = l\cos\phi_1\cos\phi_2\sin\phi_3 \qquad \phi_3 = \arctan\left(\frac{x_3}{\sqrt{x_4^2+x_5^2}}\right) \tag{2.30}$$

$$x_4 = l\cos\phi_1\cos\phi_2\cos\phi_3\sin\phi_4 \qquad \phi_4 = \arctan\left(\frac{x_4}{x_5}\right) \tag{2.31}$$

$$x_5 = l\cos\phi_1\cos\phi_2\cos\phi_3\cos\phi_4 \tag{2.32}$$

We can calculate the metric in these coordinates to find

$$\frac{ds^2}{l^2} = d\phi_1^2 + \cos^2\phi_1[d\phi_2^2 + \cos^2\phi_2(d\phi_3^2 + \cos^2\phi_3 d\phi_4^2)] \tag{2.33}$$

Changing now to de-Sitter geometry, we simply change our embedding space to Minkowski spacetime $\mathbb{R}^{1,2}$, with metric $ds^2 = -dx_0^2 + dx_i^2$, and we change our embedding surface to a hyperboloid

$$-x_0^2 + \sum_{i=1}^{4} x_i^2 = l^2 \tag{2.34}$$

With the obvious choice of coordinate transformation $x_0 \to it$, (2.34) becomes the equation for a sphere with radius l and the Minkowski metric becomes the standard metric on $\mathbb{R}^5$. Additionally, with the coordinate transformation $\phi_1 \to iT$, we get the metric

$$\frac{ds^2}{l^2} = -dT^2 + \cosh^2 T[d\phi_2^2 + \cos^2\phi_2(d\phi_3^2 + \cos^2\phi_3 d\phi_4^2)] \tag{2.35}$$

which can be simplified under trivial coordinate transformations to give

$$ds^2 = -dT^2 + l^2\cosh^2\frac{T}{l}d\Omega_3^2 \tag{2.36}$$

where $d\Omega_3^2 \equiv d\psi^2 + \sin^2\psi(d\theta^2 + \sin^2\theta d\phi^2)$ is the round metric on the unit 3-sphere.

2.2.2 Isometries of dS_4

The manifest isometries for de-Sitter space in this system are rotations and boosts, the translations that are Killing vectors of the Minkowski space-time are lost in the embedding of the coordinates onto the hyperboloid, the Killing vectors can be represented in the form

$$x_i\partial_j - x_j\partial_i \tag{2.37}$$

$$x_0\partial_i + x_i\partial_0 \tag{2.38}$$

In the context of working in four dimensions, where i and j range from 1 to 4, the maximum number of Killing vectors is given by $\frac{4(4+1)}{2} = 10$. Since there are 4 boosts and 6 rotations, the spacetime is maximally symmetric, and these Killing vectors generate the $SO(1,4)$ group.
Although, it's possible to transform the coordinate system to match the Killing vectors used in the metric (2.36), this coordinate change doesn't provide significant additional insight into the geometry of de-Sitter space. However, it's important to note that de-Sitter space lacks translational Killing vectors, resulting in non-conservation of energy and momentum, which renders the Hamiltonian ill-defined.
In this section, we'll explore metrics for de-Sitter space in which the isometries manifestly include translations.

2.2.3 Different metrics

The metric (2.36) is referred to as the global metric, and as we saw in section **2.1.6** we can compactify our coordinates to give us a different metric (2.27) which is called the conformal metric, in dS_4 this metric is

$$ds^2 = \frac{l^2}{\cos^2\tau}(-d\tau^2 + d\Omega_3^2) \tag{2.39}$$

The compactification allows us to depict the Penrose diagram shown below.
For an observer at the south pole, the red area is the region that influences the observer and the blue area is the region which can be influenced by them. The purple area is the static path which is fully accessible to the observer and the white area is the region that is completely causally disconnected from them. Unlike the Penrose diagram for dS_2, this diagram is not topologically equivalent to a cylinder as the left and right sides of the diagram are not connected, but instead represent the poles of the 2-spheres, every interior point of the diagram is a 2-sphere, which contract from the infinite past to $\tau = 0$, and expand from $\tau = 0$ to the infinite future.
Another interesting metric to look at is the static metric, which holds a historic point of note. Around 1917, Einstein was looking for solutions to a static universe, as at the time there was no evidence for the universe expanding, he worked with de-Sitter to find that

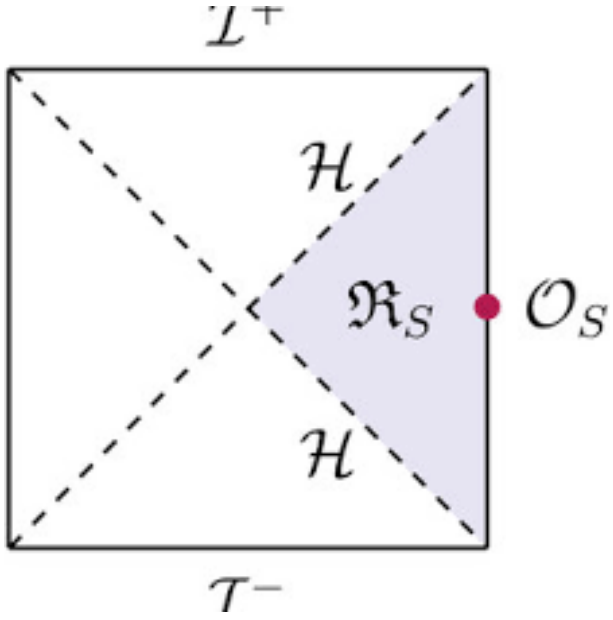

Figure 2.3: Penrose diagram dS_4

introducing the cosmological constant gave a stable solution to a static universe. Later, when it was discovered that the universe is not in fact static but expanding, he abandoned the cosmological constant, it was famously his "biggest blunder", however we now find relevance for it given the current observations showing the accelerated rate at which the universe is expanding. The metric is given by

$$ds^2 = -\left(1 - \frac{r^2}{l^2}\right) dt^2 + \left(1 - \frac{r^2}{l^2}\right)^{-1} dr^2 + r^2 d\Omega_2^2 \tag{2.40}$$

It only represents the static patch which is a quarter of the Penrose diagram from figure 2.3 shown by the purple area. We note that ∂_t is a Killing vector in these coordinates, meaning the Hamiltonian is well-defined, so the energy is a conserved quantity. We also notice that this metric appears very similar to the Schwarzschild metric, and on the null surface $r = l$, represented as the diagonal red and blue lines in figure 2.3, the norm of the Killing vector vanishes giving rise to a "cosmological horizon".

The final metric we'll look at is the one we'll use more in the later sections, as we'll see the manifest isometries give important properties to the space. The metric is referred to as the planar metric, it covers half of the global geometry. We will use the case where the metric covers the blue region from figure 2.3, a light cone emanating from a point at $\mathcal{I}^-$, however we could equally take the red region, a light cone emanating from a point at $\mathcal{I}^+$. To calculate the metric we can take the metric given by equation 2.39 and start by setting $\tilde{\eta} = \tau - \frac{\pi}{2}$ which gives

$$ds^2 = \frac{l^2}{\cos^2(\tilde{\eta} + \frac{\pi}{2})}(-d\tilde{\eta}^2 + d\Omega_3^2) \tag{2.41}$$

Then, since,

$$\cos\Big(x + \frac{\pi}{2}\Big) = -\sin(x)$$

2.41 becomes

$$ds^2 = \frac{l^2}{\sin^2\tilde{\eta}}(-d\tilde{\eta}^2 + d\Omega_3^2) \tag{2.42}$$

we, then, introduce $\eta = \lambda\tilde{\eta}$ where $\lambda \in \mathbb{R}^+$ and take the limit as $\lambda \to \infty$

$$\lim_{\lambda\to\infty} \sin\frac{\eta}{\lambda} = \frac{\eta}{\lambda}$$

which gives

$$ds^2 = \frac{l^2\lambda^2}{\eta^2}\left(-\frac{d\eta^2}{\lambda^2} + d\Omega_3^2\right) \tag{2.43}$$

We can then absorb the λ^2 term into the round metric, and we can chose a compact coordinate system for the round metric where the coordinates have both positive and negative values meaning when absorbing the λ^2 term, $\lambda^2 d\Omega_3^2$ becomes dx_i^2, the standard metric on $\mathbb{R}^3$ $(i = 1, 2, 3)$, giving the metric

$$ds^2 = \frac{l^2}{\eta^2}(-d\eta^2 + dx_i^2) \tag{2.44}$$

Looking at the ranges for the coordinates, we've already seen $x_i \in \mathbb{R}^3$, for η we find $-\frac{\pi}{2} < \tau < \frac{\pi}{2}$ gives $-\pi < \tilde{\eta} < 0$ meaning $\eta \in (-\infty, 0)$. The manifest isometries of this metric are given in the A.2 appendix of [10], we can intuitively see that spatial translations ∂_i and rotations $\epsilon_{ijk}x^i\partial^j$ are isometries as the standard metric on $\mathbb{R}^3$ features in the metric. Also if we take $\eta \to a\eta$ and $x \to ax$ where a is a constant, the metric remains unchanged therefore, dilations $-\eta\partial_\eta - x^i\partial_i$ are also an isometry. The final 3 isometries are called **special conformal transformations**, given by the Killing vectors $2x_i\eta\partial_\eta + [2x^j x_i + (\eta^2 + |\vec{x}|^2)\delta_i^j]\partial_j$. We stated earlier, that this metric will be used more in the later sections, this is because the isometries give a local property of $\mathbb{R}^3$ which allows for Fourier analysis, which we'll use to solve the Klein-Gordon equation.

2.3 de Sitter action

Let's start by considering the action

$$S = \frac{1}{16\pi G}\int d^4x\sqrt{-g}(-R) \tag{2.45}$$

we want to find the equations of motion, which we do by varying the action. Consider a matrix A, the determinant of the matrix can be written

$$\det A = e^{\operatorname{tr}\ln A} \tag{2.46}$$

which can be seen from diagonalizing A, it follows that

$$\ln \det A = \operatorname{tr} \ln A \tag{2.47}$$

$$\frac{\delta \det A}{\det A} = \operatorname{tr} \frac{\delta A}{A} \tag{2.48}$$

then for $A = g_{\mu\nu}$, $\det A = g$ we get

$$\delta g = g g^{\mu\nu} \delta g_{\mu\nu} \tag{2.49}$$

which gives

$$\delta\sqrt{-g} = -\frac{1}{2\sqrt{-g}}\delta g = -\frac{g g^{\mu\nu}\delta g_{\mu\nu}}{2\sqrt{-g}} = \frac{1}{2}\sqrt{-g} g^{\mu\nu}\delta g_{\mu\nu} = -\frac{1}{2}\sqrt{-g} g_{\mu\nu}\delta g^{\mu\nu} \tag{2.50}$$

We also need to consider the $R = R_{\mu\nu}g^{\mu\nu}$ term

$$\delta R = \delta g^{\mu\nu} R_{\mu\nu} + g^{\mu\nu}\delta R_{\mu\nu} \tag{2.51}$$

therefore, the variation of the action is

$$\delta S = -\frac{1}{16\pi G}\int d^4x\sqrt{-g}[(R_{\mu\nu} - \frac{1}{2}g_{\mu\nu}R)\delta g^{\mu\nu} + g^{\mu\nu}\delta R_{\mu\nu}] \tag{2.52}$$

The $\delta R_{\mu\nu}$ term gives a total derivative, which when integrated only gives a boundary term that can be neglected giving the equations of motion

$$R_{\mu\nu} - \frac{1}{2}g_{\mu\nu}R = 0 \tag{2.53}$$

also known as the **Einstein tensor** $G_{\mu\nu} = R_{\mu\nu} - \frac{1}{2}g_{\mu\nu}R$. Now if we add a "cosmological constant" Λ into the action given by (2.45) as follows

$$S = \frac{1}{16\pi G}\int d^4x\sqrt{-g}(2\Lambda - R) \tag{2.54}$$

It's clear to see the equations of motion become

$$R_{\mu\nu} - \frac{1}{2}g_{\mu\nu}R = -\Lambda g_{\mu\nu} \tag{2.55}$$

This is the **Einstein field equation** in a vacuum, i.e. the stress-energy tensor is zero $T_{\mu\nu} = 0$. For Minkowski space-time, the cosmological constant is zero, but for de-Sitter space-time, we require it to be positive $\Lambda > 0$. The positive constant gives rise to an expanding universe at an accelerated rate as observed [3, 11] the current approximation of the cosmological constant measured in our universe is $\Lambda \sim 10^{-122}$. We can check the metrics that we've looked at in this section obey the equations of motion (2.55) and can conclude find that $\Lambda = +3/l^2$ is greater than zero as required.

3 Classical fields in de-Sitter space

We now move on to the field theory in a de-Sitter background. Taking the Klein-Gordonn equation, we first need to alter it so that it's in the de-Sitter background and then we look at solving the equation [12]. We'll look specifically at the early and late time limits of the solution and then observe what happens for specific masses.

3.1 Klein Gordon equation

The Klein-Gordon equation is given by

$$(\Box + m^2)\phi = 0 \tag{3.1}$$

where $\Box$ is the d'Alembert operator. In flat space, it becomes $\Box = -\partial^\mu \partial_\mu$, however, as we're not in flat space, we use covariant derivatives ∇_μ instead. As, ϕ is a scalar field, the first derivative remains the same $\nabla_\mu \phi = \partial_\mu \phi$, but, then, as $\partial_\mu \phi$ is a vector quantity $\nabla^\mu \nabla_\mu \phi \neq \partial^\mu \partial_\mu \phi$. Instead, we get

$$\nabla^\mu \partial_\mu \phi = \partial^\mu \partial_\mu \phi + \Gamma^\mu_{\mu\lambda} \partial^\lambda \phi \tag{3.2}$$

Γ is the Christoffel symbol given by

$$\Gamma^k_{ij} = \frac{1}{2} g^{kl} (\partial_i g_{jl} + \partial_j g_{il} - \partial_l g_{ij}) \tag{3.3}$$

meaning

$$\Gamma^\mu_{\mu\lambda} = \frac{1}{2} g^{\mu\nu} (\partial_\lambda g_{\mu\nu} + \partial_\mu g_{\lambda\nu} - \partial_\nu g_{\mu\lambda}) = \frac{1}{2} g^{\mu\nu} \partial_\lambda g_{\mu\nu} \tag{3.4}$$

then, using the formula

$$\mathrm{Tr}(A^{-1} \partial_\lambda A) = \partial_\lambda \ln \det A \tag{3.5}$$

where A is an arbitrary matrix, we find

$$\Gamma^\mu_{\mu\lambda} = \frac{1}{2} \partial_\lambda \ln g = \frac{1}{\sqrt{g}} \partial_\lambda \sqrt{g} \tag{3.6}$$

it follows that

$$\nabla^\mu \partial_\mu \phi = (\partial^\mu \partial_\mu + \frac{1}{\sqrt{g}} \partial_\lambda \sqrt{g} \partial^\lambda) \phi = \frac{1}{\sqrt{g}} \partial_\mu (g^{\mu\nu} \sqrt{g} \partial_\nu \phi) \tag{3.7}$$

This is explained in very detail on pages 106-107 in [13]. This gives us the Klein-Gordon equation in curved space as

$$\frac{1}{\sqrt{g}} \partial_\mu (g^{\mu\nu} \sqrt{g} \partial_\nu \phi) = m^2 \phi \tag{3.8}$$

Taking the planar metric (2.44) we find

$$g_{\mu\nu} = \frac{l^2}{\eta^2}\begin{pmatrix} -1 & 0 & 0 & 0 \\ 0 & 1 & 0 & 0 \\ 0 & 0 & 1 & 0 \\ 0 & 0 & 0 & 1 \end{pmatrix} \qquad g^{\mu\nu} = \frac{\eta^2}{l^2}\begin{pmatrix} -1 & 0 & 0 & 0 \\ 0 & 1 & 0 & 0 \\ 0 & 0 & 1 & 0 \\ 0 & 0 & 0 & 1 \end{pmatrix} \tag{3.9}$$

this also gives us

$$g = -\frac{l^8}{\eta^8} \qquad \sqrt{-g} = \frac{l^4}{\eta^4} \tag{3.10}$$

(we need not concern ourselves with the minus sign in $\sqrt{-g}$) substituting (3.10) into (3.8) gives us

$$\frac{\eta^4}{l^4}\partial_\eta(-\frac{l^2}{\eta^2}\partial_\eta\phi) + \frac{\eta^4}{l^4}\partial_{\vec{x}}(\frac{l^2}{\eta^2}\partial_{\vec{x}}\phi) = m^2\phi \tag{3.11}$$

which simplifies to

$$[-\eta^4\partial_\eta(\eta^{-2}\partial_\eta) + \eta^2\partial_{\vec{x}}^2]\phi = m^2l^2\phi \tag{3.12}$$

As stated earlier, we can use a Fourier transformation to solve this differential equation, which we're able to do because of the local property of $\mathbb{R}^3$ on the planar metric. Note that, the momentum $\vec{k}$ that we're doing the Fourier decomposition with respect to is not the physical momentum, but is actually a coordinate momentum and the physical momentum is $\vec{k}_{phys} = \eta\vec{k}$. Using the Fourier transform

$$\phi(\eta, \vec{x}) = \int \frac{d^3k}{(2\pi)^3} e^{i\vec{k}\cdot\vec{x}}\phi(\eta, \vec{k}) \tag{3.13}$$

equation (3.12) becomes

$$[\eta^4\partial_\eta(\eta^{-2}\partial_\eta) + \eta^2k^2 + m^2l^2]\phi(\eta, \vec{k}) = 0 \tag{3.14}$$

where $k = \sqrt{\vec{k}^2}$. The solution to this equation is given in Appendix as

$$\phi_1(\eta, \vec{k}) = A(\vec{k})\eta^{3/2}\mathcal{J}_\nu(\eta k) \tag{3.15}$$

$$\phi_2(\eta, \vec{k}) = B(\vec{k})\eta^{3/2}\mathcal{Y}_\nu(\eta k) \tag{3.16}$$

where $\nu^2 = 9/4 - m^2l^2$, $A(\vec{k})$ and $B(\vec{k})$ are arbitrary functions, and $\mathcal{J}_\nu(x)$ and $\mathcal{Y}_\nu(x)$ are the Bessel functions of first and second kind respectively. We can combine our two solutions and substitute back into (3.13) to give a general solution

$$\phi(\eta, \vec{x}) = \int \frac{d^3k}{(2\pi)^3}\left[A(\vec{k})\mathcal{J}_\nu(\eta k) + B(\vec{k})\mathcal{Y}_\nu(\eta k)\right]\eta^{3/2}e^{i\vec{k}\cdot\vec{x}} \tag{3.17}$$

The Bessel functions themselves are not simple to express, the most common way is a series expansion given by

$$\mathcal{J}_\nu(z) = \left(\frac{z}{2}\right)^\nu \sum_{k=0}^{\infty} (-1)^k \frac{(\frac{1}{4}z^2)^k}{k!\Gamma(\nu+k+1)} \tag{3.18}$$

$$\mathcal{Y}_\nu(z) = \frac{\mathcal{J}_\nu(z)\cos(\nu\pi) - \mathcal{J}_{-\nu}(z)}{\sin(\nu\pi)} \tag{3.19}$$

Because of the complexity in expressing these solutions, we'll find it more accessible to review specific areas of the solution, where it's expressed in a comprehensible manner. As such, in the next sections we proceed by reviewing the limiting behavior of the Bessel functions corresponding to the early and late time limits and then look to some specific values for ν, which we notice assumes a complex value when $ml > 3/2$, and as we require $\phi(\eta, \vec{x})$ to be real, the functions $A(\vec{k})$ and $B(\vec{k})$ will become complex too.
We note that, when we come to quantizing the field later on, we'll want to have defined the conjugate momentum. So, we now go about the calculation to find the conjugate momentum, we start by identifying the action for the Klein-Gordon equation is

$$S = -\frac{1}{2}\int d^4x\sqrt{-g}(g^{\mu\nu}\partial_\mu\phi\partial_\nu\phi + m^2\phi^2) \tag{3.20}$$

from this. we get the Lagrangian density

$$\mathcal{L} = -\frac{1}{2}\sqrt{-g}(g^{\mu\nu}\partial_\mu\phi\partial_\nu\phi + m^2\phi^2) = \frac{l^2}{2\eta^2}(\partial_\eta\phi)^2 - \frac{l^2}{2\eta^2}(\partial_{\vec{x}}\phi)^2 - \frac{l^4}{2\eta^4}m^2\phi^2 \tag{3.21}$$

We note that this technically is not a true Lagrangian density as the $\vec{x}$ coordinates are not the proper spatial lengths because η weighs the proper length. With the following definition of the conjugate momentum

$$\pi(\eta, \vec{x}) = \frac{\partial\mathcal{L}}{\partial(\partial_\eta\phi)}$$

we find

$$\pi(\eta, \vec{x}) = \frac{l^2}{\eta^2}\partial_\eta\phi \tag{3.22}$$

using this, we can also calculate the Hamiltonian density

$$\mathcal{H} = \pi\partial_\eta\phi - \mathcal{L} = \frac{l^2}{2\eta^2}(\partial_\eta\phi)^2 + \frac{l^2}{2\eta^2}(\partial_{\vec{x}}\phi)^2 + \frac{l^4}{2\eta^4}m^2\phi^2 \tag{3.23}$$

we see that, it has an explicit time dependence and therefore the energy is not conserved which agrees with our earlier finding that the time translations ∂_t are not Killing vectors of the global geometry.

3.2 Solution to early time limit

We look first at the early time limit where $|\eta| \to \infty$, from [14] we see that

$$\mathcal{J}_\nu(z) \sim \sqrt{\frac{2}{\pi z}} \cos(z - \Phi) \tag{3.24}$$

$$\mathcal{Y}_\nu(z) \sim \sqrt{\frac{2}{\pi z}} \sin(z - \Phi) \tag{3.25}$$

where, $\Phi = \frac{1}{2}\nu\pi + \frac{1}{4}\pi$ is a constant phase. We notice the behavior is oscillatory for early times, but before substituting it into our general solution we notice that a more appealing form can be seen when changing to the Hankel functions

$$\mathcal{J}_\nu(z) + i\mathcal{Y}_\nu(z) = H_\nu^{(1)}(z) \underset{z\to\infty}{\sim} \sqrt{\frac{2}{\pi z}} e^{i(z-\Phi)} \tag{3.26}$$

$$\mathcal{J}_\nu(z) - i\mathcal{Y}_\nu(z) = H_\nu^{(2)}(z) \underset{z\to\infty}{\sim} \sqrt{\frac{2}{\pi z}} e^{-i(z-\Phi)} \tag{3.27}$$

we can now substitute these approximations into our general solution to get the behaviour of early time limit as

$$\phi(\eta, \vec{x}) = \int \frac{d^3k}{(2\pi)^3} \left[a(\vec{k})\eta \sqrt{\frac{2}{\pi k}} e^{i(\eta k - \Phi + \vec{k}\cdot\vec{x})} + b(\vec{k})\eta \sqrt{\frac{2}{\pi k}} e^{-i(\eta k - \Phi - \vec{k}\cdot\vec{x})} \right] \tag{3.28}$$

where $a(\vec{k})$ and $b(\vec{k})$ are functions of $A(\vec{k})$ and $B(\vec{k})$, and as we require $\phi(\eta, \vec{x})$ to be real $a^*(\vec{k}) = b(-\vec{k})$ giving

$$\phi(\eta, \vec{x}) = \int \frac{d^3k}{(2\pi)^3} \eta \sqrt{\frac{2}{\pi k}} \left[a(\vec{k}) e^{i(\eta k - \Phi + \vec{k}\cdot\vec{x})} + a^*(\vec{k}) e^{-i(\eta k - \Phi + \vec{k}\cdot\vec{x})} \right] \tag{3.29}$$

This looks very similar to the solution to the Klein Gordon equation in flat space only multiplied by a factor of η (although we note η is not the proper time), meaning for the far past the scalar field has a similar solution to that of flat space.

3.3 Solution to late time limit

We can now look at the late time limit $\eta \to 0$, from [14] we find [1]

$$\mathcal{J}_\nu(z) \sim \frac{(\frac{1}{2}z)^\nu}{\Gamma(\nu + 1)} \tag{3.30}$$

$$\mathcal{Y}_\nu(z) \sim -\frac{1}{\pi}\Gamma(\nu)(\frac{1}{2}z)^{-\nu} \tag{3.31}$$

[1] These two papers [15, 16] have some interesting discussions of the late-time behaviour of **Bunch-Davies FRW wavefunction**.

substituting these approximations into our general solution to get the late time behaviour gives

$$\phi(\eta,\vec{x}) = \int \frac{d^3k}{(2\pi)^3}\eta^{3/2}e^{i\vec{k}\cdot\vec{x}}\left(A(\vec{k})\frac{(\frac{1}{2}\eta k)^\nu}{\Gamma(\nu+1)} - B(\vec{k})\frac{\Gamma(\nu)}{\pi(\frac{1}{2}\eta k)^\nu}\right) \tag{3.32}$$

Another approach to solving the late time limit is to take the limit $\eta \to 0$ of the differential equation (3.12). Following the solution from the lecture [17, 18] we find, when we take the limit $\eta \to 0$ the $\eta^2\partial_{\vec{x}}^2$ term is subleading, leaving us with an ordinary differential equation which is a lot easier to solve than the partial differential equation we have already worked through. We'll now work through the solution to the following ODE

$$-\eta^4\partial_\eta(\eta^{-2}\partial_\eta)\phi(\eta,\vec{x}) = m^2l^2\phi(\eta,\vec{x}) \tag{3.33}$$

we propose an ansatz for the solution to be of the form

$$\phi(\eta,\vec{x}) = \eta^\kappa a(\vec{x}) \tag{3.34}$$

where, $\kappa \in \mathbb{C}$ is a constant and as (3.33) is an ODE the solution can include an arbitrary function of $\vec{x}$. Substituting (3.34) into (3.33) gives

$$-\kappa(\kappa-3)\eta^\kappa a(\vec{x}) = m^2l^2\eta^\kappa a(\vec{x}) \tag{3.35}$$

giving the algebraic equation

$$\kappa^2 - 3\kappa + m^2l^2 = 0 \tag{3.36}$$

which has solutions

$$\kappa_\pm = \frac{3}{2} \pm \sqrt{\frac{9}{4} - m^2l^2} \tag{3.37}$$

we can then substitute this into (3.34) to give the general solution

$$\phi(\eta,\vec{x}) = \eta^{\kappa_+}a_+(\vec{x}) + \eta^{\kappa_-}a_-(\vec{x}) + ... \tag{3.38}$$

The +... at the end implies we've not got the complete solution, for example when $m^2l^2 = \frac{9}{4}$, κ is single-valued, hence there'd appear a log term to account for the degeneracy, however for our discussion we need not concern ourselves with the missing solutions. What we're interested in is how this solution behaves for different masses which will be covered in the following section.

3.4 Solutions to different masses

If we now take a closer look at specific masses for the solution to the late time limit equation (3.38), we see that for particles with large masses $ml >> \frac{3}{2}$, κ is complex-valued, intuitively we can regard heavy particles moving through the space-time, as not sensing the curvature of the space-time that much. It is this fact that κ becomes complex for large masses that proves this intuition as it means that even in the late time limit the particle retains an oscillatory behaviour, bearing in mind that η is not the proper time when expressed in the terms of proper time $\eta = -e^{-T/l}$ where T is the proper time. This oscillatory behaviour stops at the critical mass $m_c l = \frac{3}{2}$ where $\kappa_+ = \kappa_-$, at this point instead of the oscillatory behavior we are familiar with the solutions decay exponentially. The exponential decay of both modes is also the solution seen in the range $0 < ml < \frac{3}{2}$. However, for the case, where the particle is massless, $\kappa_- = 0$ meaning one of the modes is not decaying exponentially, but leaves an imprint for arbitrarily late times, and it's this feature that allows us to have any chance of observing scale-invariant fluctuations from the early cosmological era.

4 Quantum fields in de Sitter space

Having gained an understanding of the classical scalar field, we move onto quantizing the field [19, 20]. Our procedure will follow that of canonical quantization, however, we notice that with the mode expansion of the classical field solution not being unique, we've got a choice to make that affects how we define our vacuum state. We will use the mode expansion from equation (3.29) meaning when $a(\vec{k})$ acts on the vacuum state, it is annihilated.

4.1 Quantization

To quantize our field we promote $\phi(\eta, \vec{x})$ and $\pi(\eta, \vec{x})$ to operators obeying the commutation relations

$$[\phi(\eta, \vec{x}), \phi(\eta, \vec{y})] = 0 \tag{4.1}$$

$$[\pi(\eta, \vec{x}), \pi(\eta, \vec{y})] = 0 \tag{4.2}$$

$$[\phi(\eta, \vec{x}), \pi(\eta, \vec{y})] = i\delta^{(3)}(\vec{x} - \vec{y}) \tag{4.3}$$

the coefficients $a(\vec{k})$ and $a^*(\vec{k})$ are also promoted to operators and obey the commutation relations

$$[a(\vec{k}), a(\vec{k'})] = 0 \tag{4.4}$$

$$[a^\dagger(\vec{k}), a^\dagger(\vec{k'})] = 0 \tag{4.5}$$

$$[a(\vec{k}), a^\dagger(\vec{k'})] = (2\pi)^3\delta^{(3)}(\vec{k} - \vec{k'}) \tag{4.6}$$

and we have that $a(\vec{k})\,|0\rangle = 0$, which allows us to generate the Fock space in the same way we would in flat space. Now using equation (3.17) and following a similar procedure that lead to the equation (3.29) we get

$$\phi(\eta, \vec{x}) = \int \frac{d^3k}{(2\pi^3)}\eta^{3/2}[a(\vec{k})e^{i\vec{k}\cdot\vec{x}}H_\nu^{(1)}(\eta k) + a^\dagger(\vec{k})e^{-i\vec{k}\cdot\vec{x}}H_\nu^{(2)}(\eta k)] \tag{4.7}$$

we can separate this into the creation and annihilation parts which we will use in the calculation of the two point function

$$\phi^-(\eta, \vec{x}) = \int \frac{d^3k}{(2\pi^3)}\eta^{3/2}a(\vec{k})e^{i\vec{k}\cdot\vec{x}}H_\nu^{(1)}(\eta k) \tag{4.8}$$

$$\phi^+(\eta, \vec{x}) = \int \frac{d^3k}{(2\pi^3)}\eta^{3/2}a^\dagger(\vec{k})e^{-i\vec{k}\cdot\vec{x}}H_\nu^{(2)}(\eta k) \tag{4.9}$$

4.2 Two point function

We finally get to calculating the two point function [21, 22]

$$\langle 0|\, \phi(\eta, \vec{x})\phi(\eta', \vec{y})\, |0\rangle \tag{4.10}$$

by definition

$$\phi(\eta, \vec{x})\phi(\eta', \vec{y}) =: \phi(\eta, \vec{x})\phi(\eta', \vec{y}) : +[\phi^-(\eta, \vec{x}), \phi^+(\eta', \vec{y})] \tag{4.11}$$

the colons represent normal ordering, where the annihilation operators are moved to the right, meaning when this is substituted into (4.10) it gives us

$$\langle 0|\, [\phi^-(\eta, \vec{x}), \phi^+(\eta', \vec{y})]\, |0\rangle \tag{4.12}$$

$$= \eta^{3/2}\eta'^{3/2} \int \frac{d^3k}{(2\pi)^3}\frac{d^3k'}{(2\pi)^3} H_\nu^{(1)}(\eta k) H_\nu^{(2)}(\eta' k') e^{i(\vec{k}\cdot\vec{x} - \vec{k'}\cdot\vec{y})} \langle 0|\, [a(\vec{k}), a^\dagger(\vec{k'})]\, |0\rangle \tag{4.13}$$

substituting in the relation (4.6) and integrating over the k' coordinate gives us

$$\langle 0|\, \phi(\eta, \vec{x})\phi(\eta', \vec{y})\, |0\rangle = (\eta\eta')^{3/2} \int \frac{d^3k}{(2\pi)^3} H_\nu^{(1)}(\eta k) H_\nu^{(2)}(\eta' k) e^{i\vec{k}\cdot(\vec{x} - \vec{y})} \tag{4.14}$$

As this is not an easy integral to solve, we can again look at the approximation of the solution in the early and late time limits. Before we change to the limiting behavior we can look at changing to spherical polar coordinates to perform the integration, in doing so we use $\vec{a}\cdot\vec{b} = |a||b|\cos\theta$, where $\vec{a}$ and $\vec{b}$ are vectors and θ is the angle between them, we get

$$\langle 0|\, \phi(\eta, \vec{x})\phi(\eta', \vec{y})\, |0\rangle = \frac{(\eta\eta')^{3/2}}{(2\pi)^3} \int_0^\infty dr \int_0^{2\pi} d\phi \int_0^\pi d\theta r^2 \sin\theta H_\nu^{(1)}(\eta r) H_\nu^{(2)}(\eta' r) e^{ir|\vec{x} - \vec{y}|\cos\theta} \tag{4.15}$$

then, doing the integral over $d\phi$ gives a factor of 2π, we'll calculate the integral over $d\theta$ which leaves us with

$$\langle 0|\, \phi(\eta, \vec{x})\phi(\eta', \vec{y})\, |0\rangle = \frac{2}{|\vec{x} - \vec{y}|} \frac{(\eta\eta')^{3/2}}{(2\pi)^2} \int_0^\infty dr r \sin(r|\vec{x} - \vec{y}|) H_\nu^{(1)}(\eta r) H_\nu^{(2)}(\eta' r) \tag{4.16}$$

It is at this point that the integral becomes too complicated to solve without taking the early and late time limits, we'll start by considering the early time limit where the Hankel functions are approximated by equations (3.26) and (3.27) which gives

$$\langle 0|\, \phi(\eta, \vec{x})\phi(\eta', \vec{y})\, |0\rangle = \frac{8}{|\vec{x} - \vec{y}|} \frac{(\eta\eta')}{(2\pi)^3} \int_0^\infty dr \sin(r|\vec{x} - \vec{y}|) e^{ir(\eta - \eta')} \tag{4.17}$$

Now, we'll solve this integral to give us the final solution for the two-point function in the early time limit as

$$\langle 0|\,\phi(\eta,\vec{x})\phi(\eta',\vec{y})\,|0\rangle = \frac{8}{|\vec{x}-\vec{y}|}\frac{(\eta\eta')}{(2\pi)^3}\frac{|\vec{x}-\vec{y}|}{|\vec{x}-\vec{y}|^2-(\eta-\eta')^2} = \frac{1}{\pi^3}\frac{\eta\eta'}{|\vec{x}-\vec{y}|^2-(\eta-\eta')^2} \tag{4.18}$$

Now, we can look at specific cases of $x-y$, we see for a time-like interval $\vec{x}-\vec{y}=0$ and $\eta-\eta'=t$, we get

$$\langle 0|\,\phi(\eta,\vec{x})\phi(\eta',\vec{y})\,|0\rangle = -\frac{1}{\pi^3}\frac{\eta\eta'}{t^2} \tag{4.19}$$

Comparing this to the solution in flat space given the limit
$t\to\infty$ has the approximate solution e^{-imt}. We can also look at the space-like interval $\vec{x}-\vec{y}=r$ and $\eta-\eta'=0$, we get

$$\langle 0|\,\phi(\eta,\vec{x})\phi(\eta',\vec{y})\,|0\rangle = \frac{1}{\pi^3}\frac{\eta\eta'}{|\vec{x}-\vec{y}|^2} \tag{4.20}$$

We compare this to our solution in flat space given the limit $r\to\infty$ which has the approximate solution e^{-mr}.
We now move onto the late time limit, we first need to find the limiting behavior of the Hankel functions. We take the limits of the Bessel functions from equations (3.30) and (3.31) and change to the form of the Hankel functions using the relations seen in (3.26) and (3.27) which gives

$$H_\nu^{(1)}(z) \sim \frac{(\frac{1}{2}z)^\nu}{\Gamma(\nu+1)} - \frac{i}{\pi}\frac{\Gamma(\nu)}{(\frac{1}{2}z)^\nu} \tag{4.21}$$

$$H_\nu^{(2)}(z) \sim \frac{(\frac{1}{2}z)^\nu}{\Gamma(\nu+1)} + \frac{i}{\pi}\frac{\Gamma(\nu)}{(\frac{1}{2}z)^\nu} \tag{4.22}$$

From equation, (4.16) we want to calculate $H_\nu^{(1)}(\eta r)H_\nu^{(2)}(\eta' r)$ which gives

$$\frac{(\frac{1}{2}k)^{2\nu}(\eta\eta')^\nu}{\Gamma^2(\nu+1)} + \frac{i}{\pi\nu}(\frac{\eta}{\eta'})^\nu - \frac{i}{\pi\nu}(\frac{\eta'}{\eta})^\nu + \frac{1}{\pi^2}\frac{\Gamma^2(\nu)}{(\frac{1}{2}k)^{2\nu}(\eta\eta')^\nu} \tag{4.23}$$

however, in the limit $\eta\to 0$ the first three terms are subleading so can be disregarded, giving us

$$\langle 0|\,\phi(\eta,\vec{x})\phi(\eta',\vec{y})\,|0\rangle = \frac{2}{|\vec{x}-\vec{y}|}\frac{(\eta\eta')^{3/2}}{(2\pi)^2}\int_0^\infty dr r\sin(r|\vec{x}-\vec{y}|)\frac{1}{\pi^2}\frac{\Gamma^2(\nu)}{(\frac{1}{2}r)^{2\nu}(\eta\eta')^\nu} \tag{4.24}$$

simplifying to give

$$\langle 0|\,\phi(\eta,\vec{x})\phi(\eta',\vec{y})\,|0\rangle = \frac{2^{(2+2\nu)}}{|\vec{x}-\vec{y}|}\frac{(\eta\eta')^{3/2-\nu}}{(2\pi)^3}\frac{\Gamma^2(\nu)}{\pi}\int_0^\infty dr r^{1-2\nu}\sin(r|\vec{x}-\vec{y}|) \tag{4.25}$$

Solving this integral,

$$\langle 0|\,\phi(\eta,\vec{x})\phi(\eta',\vec{y})\,|0\rangle = \frac{2^{(2+2\nu)}}{|\vec{x}-\vec{y}|}\frac{(\eta\eta')^{3/2-\nu}}{(2\pi)^3}\frac{\Gamma^2(\nu)}{\pi}|\vec{x}-\vec{y}|^{2\nu-2}\Gamma(2-2\nu)\sin(\pi\nu) \tag{4.26}$$

$$= \frac{2^{(2+2\nu)}}{\pi}\frac{\sin(\pi\nu)}{(2\pi)^3}\Gamma^2(\nu)\Gamma(2-2\nu)|\vec{x}-\vec{y}|^{2\nu-3}(\eta\eta')^{3/2-\nu} \tag{4.27}$$

$$= f(\nu)|\vec{x}-\vec{y}|^{2\nu-3}(\eta\eta')^{3/2-\nu} \tag{4.28}$$

where function $f(\nu)$ simplifies the appearance of the solution. However, it is important to note that this solution is conditional and holds true only for the range of $\frac{1}{2} < \mathrm{Re}(\nu) < \frac{3}{2}$. If we focus on the timelike interval where $\vec{x}-\vec{y}=0$ and $\eta-\eta'=t$, we obtain the following expression

$$\langle 0|\,\phi(\eta,\vec{x})\phi(\eta',\vec{y})\,|0\rangle = f(\nu)(\eta\eta')^{3/2-\nu} \tag{4.29}$$

We also note that for the massless particle $\nu = \frac{3}{2}$, although the function $f(\nu)$ is not analytic at this point, we notice that the solution has no explicit time dependence or spatial separation dependence, meaning the correlations do not dilute with time, which gives cosmologists a chance of observing the fluctuations from the inflationary era.

5 Conclusion

In summary, the paper extensively examines the geometry of the de Sitter background, particularly focusing on the isometries of the spacetime. It reveals that the lack of ∂_t as a Killing vector in the global geometry results in the non-conservation of energy. This observation is further supported by the explicit time dependence of the Hamiltonian.
By solving, the classical Klein-Gordon equation, the paper discovers that even in the late-time limit, where particles have significant mass ($ml > \frac{3}{2}$), the solutions exhibit oscillatory behavior. This finding challenges the notion that massive particles in the late-time de-Sitter space-time would exhibit non-oscillatory behavior.
The paper concludes by quantizing the field and comparing the solutions obtained with those in flat space-time. An important discovery is made concerning massless particles: their correlations do not dilute with time, opening up the possibility for observations from the inflationary era of our universe. The paper suggests that further exploration could involve investigating an interacting theory, such as the three-point function, which has not been explored in this particular study.

Appendix

This appendix follows the solution to the differential equation (3.14). We first expand the equation to give

$$[\eta^2\partial_\eta^2 - 2\eta\partial_\eta + \eta^2k^2 + m^2l^2]\phi(\eta,\vec{k}) = 0$$

We identify that the solutions to this are going to be Bessel functions, as such we look for transformations that get the equation into the form

$$[x^2\partial_x^2 + x\partial_x + (x^2 - \alpha^2)]y(x) = 0$$

and make a transformation to the field $\phi = \eta^{3/2}\tilde{\phi}$ which gives

$$[\eta^2\partial_\eta^2 - 2\eta\partial_\eta + \eta^2k^2 + m^2l^2]\eta^{3/2}\tilde{\phi}(\eta,\vec{k}) = 0$$

and is solved to give

$$\eta^{7/2}\partial_\eta^2\tilde{\phi}(\eta,\vec{k}) + \eta^{5/2}\partial_\eta\tilde{\phi}(\eta,\vec{k}) - \frac{9}{4}\eta^{3/2}\tilde{\phi}(\eta,\vec{k}) + (\eta^2k^2 + m^2l^2)\eta^{3/2}\tilde{\phi}(\eta,\vec{k}) = 0$$

Now, if we divide through by $\eta^{3/2}$, we get

$$[\eta^2\partial_\eta^2 + \eta\partial_\eta + (-\frac{9}{4} + \eta^2k^2 + m^2l^2)]\tilde{\phi}(\eta,\vec{k}) = 0$$

Makingthe change of coordinates $\tilde{\eta} = \eta k$, we find

$$\partial_\eta = \partial_{\tilde{\eta}}\frac{d\tilde{\eta}}{d\eta} = k\partial_{\tilde{\eta}}$$

that gives

$$[\tilde{\eta}^2\partial_{\tilde{\eta}}^2 + \tilde{\eta}\partial_{\tilde{\eta}} + (\tilde{\eta}^2 + m^2l^2 - \frac{9}{4})]\tilde{\phi}(\tilde{\eta},\vec{k}) = 0$$

which is of the form of the Bessel equation, so, if we set $\nu^2 = \frac{9}{4} - m^2l^2$, our solutions are

$$\tilde{\phi}_1(\tilde{\eta},\vec{k}) = A(\vec{k})\mathcal{J}_\nu(\tilde{\eta})$$

$$\tilde{\phi}_2(\tilde{\eta},\vec{k}) = B(\vec{k})\mathcal{Y}_\nu(\tilde{\eta})$$

which, when we convert back to our original form gives us the solutions to equation (3.14) as

$$\phi_1(\eta,\vec{k}) = A(\vec{k})\eta^{3/2}\mathcal{J}_\nu(\eta k)$$

$$\phi_2(\eta,\vec{k}) = B(\vec{k})\eta^{3/2}\mathcal{Y}_\nu(\eta k)$$

References

[1] S. Perlmutter, G. Aldering, G. Goldhaber, R. A. Knop, P. Nugent, P. G. Castro, S. Deustua, S. Fabbro, A. Goobar, D. E. Groom, I. M. Hook, A. G. Kim, M. Y. Kim, J. C. Lee, N. J. Nunes, R. Pain, C. R. Pennypacker, R. Quimby, C. Lidman, R. S. Ellis, M. Irwin, R. G. McMahon, P. Ruiz-Lapuente, N. Walton, B. Schaefer, B. J. Boyle, A. V. Filippenko, T. Matheson, A. S. Fruchter, N. Panagia, H. J. M. Newberg, W. J. Couch, and The Supernova Cosmology Project. Measurements of Ω and Λ from 42 high-redshift supernovae. *The Astrophysical Journal*, 517(2):565–586, jun 1999.

[2] Adam G. Riess, Alexei V. Filippenko, Peter Challis, Alejandro Clocchiatti, Alan Diercks, Peter M. Garnavich, Ron L. Gilliland, Craig J. Hogan, Saurabh Jha, Robert P. Kirshner, B. Leibundgut, M. M. Phillips, David Reiss, Brian P. Schmidt, Robert A. Schommer, R. Chris Smith, J. Spyromilio, Christopher Stubbs, Nicholas B. Suntzeff, and John Tonry. Observational evidence from supernovae for an accelerating universe and a cosmological constant. *The Astronomical Journal*, 116(3):1009–1038, sep 1998.

[3] Raphael Bousso. The cosmological constant. *General Relativity and Gravitation*, 40(2-3):607–637, dec 2007.

[4] Kentaro Nagamine and Abraham Loeb. Future evolution of nearby large-scale structures in a universe dominated by a cosmological constant. *New Astronomy*, 8(5):439–448, jul 2003.

[5] Daniel Baumann. Tasi lectures on inflation, 2012.

[6] Shinji Tsujikawa. Introductory review of cosmic inflation, 2003.

[7] Yoonbai Kim, Chae Young Oh, and Namil Park. Classical geometry of de sitter spacetime : An introductory review, 2002.

[8] Mu-Lin Yan. Killing vectors in spacetime of the de sitter invariant special relativity, 2017.

[9] Thomas Hartman. Lecture notes on classical de sitter space. Year.

[10] Gizem Şengör and Constantinos Skordis. Unitarity at the late time boundary of de sitter. *Journal of High Energy Physics*, 2020(6), jun 2020.

[11] John D. Barrow and Douglas J. Shaw. The value of the cosmological constant. *General Relativity and Gravitation*, 43(10):2555–2560, jun 2011.

[12] Karen Yagdjian and Anahit Galstyan. Fundamental solutions for the klein-gordon equation in de sitter spacetime. *Communications in Mathematical Physics*, 285:293–344, 10 2009.

[13] Steven Weinberg. *Gravitation and Cosmology: Principles and Applications of the General Theory of Relativity*. Wiley, 1972.

[14] F. W. J. Olver and A. B. Olde Daalhuis and D. W. Lozier and B. I. Schneider and R. F. Boisvert and C. W. Clark and B. R. Miller and B. V. Saunders and H. S. Cohl and M. A. McClain. *NIST Digital Library of Mathematical Functions*. https://dlmf.nist.gov/, Release 1.1.10 of 2023-06-15. Edited by F. W. J. Olver et al.

[15] George Konstantinidis, Raghu Mahajan, and Edgar Shaghoulian. Late-time structure of the bunch-davies FRW wavefunction. *Journal of High Energy Physics*, 2016(10), oct 2016.

[16] Dionysios Anninos, Tarek Anous, Daniel Z. Freedman, and George Konstantinidis. Late-time structure of the bunch-davies de sitter wavefunction. *Journal of Cosmology and Astroparticle Physics*, 2015(11):048, nov 2015.

[17] Dionysios Anninos. Aspects of de sitter space, 2018.

[18] Dionysios Anninos. Topics in de sitter space, 2018.

[19] DIONYSIOS ANNINOS. DE SITTER MUSINGS. *International Journal of Modern Physics A*, 27(13):1230013, may 2012.

[20] E. T. Akhmedov. Lecture notes on interacting quantum fields in de Sitter space. *Int. J. Mod. Phys. D*, 23:1430001, 2014.

[21] T. S. Bunch and P. C. W. Davies. Quantum field theory in de sitter space: Renormalization by point-splitting. *Proceedings of the Royal Society of London. Series A, Mathematical and Physical Sciences*, 360(1700):117–134, 1978.

[22] E. T. Akhmedov, K. V. Bazarov, D. V. Diakonov, and U. Moschella. Quantum fields in the static de sitter universe. *Physical Review D*, 102(8), oct 2020.